Liquid Crystals
Publication details, including instructions for authors and subscription information:
http://www.informaworld.com/smpp/title~content=t713926090

Melting and spherulitic crystallization of a phenyl benzoate

K. S. Krishnamurthy[a]
[a] Department of Applied Sciences, Faculty of Electrical and Mechanical Engineering, College of Military Engineering, Pune, India

To cite this Article Krishnamurthy, K. S.(1991) 'Melting and spherulitic crystallization of a phenyl benzoate', Liquid Crystals, 9: 5, 727 — 739
To link to this Article: DOI: 10.1080/02678299108030385
URL: http://dx.doi.org/10.1080/02678299108030385

LIQUID CRYSTALS, 1991, VOL. 9, NO. 5, 727–739

Melting and spherulitic crystallization of a phenyl benzoate

by K. S. KRISHNAMURTHY
Department of Applied Sciences, Faculty of Electrical and Mechanical Engineering, College of Military Engineering, Pune 411 031, India

(*Received 12 February 1990; accepted 12 December 1990*)

Melting and solidification of BPC (butyl *p*-(*p*-ethoxyphenoxycarbonyl)phenylcarbonate) have been studied by polarization microscopy and differential scanning calorimetry. BPC can exist at room temperature in two different crystallographic modifications which melt directly into the nematic state at different temperatures (*c.* 330·5 K and 338·5 K). The nematic fluid crystallizes below *c.* 313 K to form simultaneously two types of spherulitic aggregates corresponding to the two crystal types. Both the spherulites possess a positive birefringence; but they vary significantly in their morphological and kinetic aspects. Further, in one of them the molecular long axes are radial, while in the other they are tangential. This fact emerges from optical and electrooptical observations on the pseudomorphic nematic domains obtained by melting the spherulites. Above 313 K, the crystals that grow are nonspherulitic, lamellar, biaxial and optically positive; they melt at *c.* 338·5 K. The glassy nematic state is realised by rapidly quenching the melt to a low temperature (100 K). On heating, the glassy state transforms into the supercooled nematic state near 234·5 K.

1. Introduction

Spherulitic organization is often a distinctive feature of the growth of anisotropic crystallites from considerably undercooled, viscous melts [1–3]. Mesomorphic melts could therefore be expected, in many cases, to crystallize as spherulites. However, while there have been numerous investigations of spherulitic aggregation in non-mesomorphic materials [1, 2], relatively little is known of liquid crystals in this field [4]. The few detailed reports that are available [5–10] relate mainly to the kinetics of spherulite evolution from the cholesteric and smectic phases of some cholesteryl esters. As for nematogens, there have only been some brief references to spherulitic aggregation in some azoxy compounds [11, 12]. Morphological aspects remain largely unexplored for all classes of liquid crystals. Thus, when we observed nematic BPC ($C_4H_9O.CO.O.C_6H_4.CO.O.C_6H_4.OC_2H_5$) crystallizing into spherulitic structures (unlike several other phenyl benzoates [13, 14]), it appeared of interest to carry out a systematic study of this crystallization process. Additionally, on observing that these structures melted to give paramorphic nematic domains, it seemed worthwhile to extend our previous electric field experiments [15, 16] to these novel director configurations. The results presented here are from optical studies, complemented by DSC and X-ray measurements.

2. Experimental

The sample of BPC used was from Eastman Kodak Co. and of purity over 99 per cent as estimated by gas chromatography. The textures were examined in transmitted light using Carl Zeiss and Ernst Leitz Wetzlar polarizing microscopes. White light was

0267–8292/91 $3·00

used, except in interference studies for which mercury green was employed. The specimens were held between glass plates separated by 75 μm teflon spacers. For electric field experiments, the plates were tin oxide coated and the field frequency was 30–100 Hz in the conduction regime and 10 kHz in the dielectric regime. The voltages given are the rms values. For determining the transition temperatures, an electrically heated stage was used. It was similar to that described by Gray [17], except for the use of a copper constantan thermocouple in place of a thermometer. It could be maintained at the desired temperature to an accuracy of $\pm 0{\cdot}1$°C. For isothermal studies (in the range 278–325 K), a separate stage was used. It was essentially an insulated copper block with a slide slot; its temperature was controlled to an accuracy of $\pm 0{\cdot}3$°C, by circulating thermostatted water through it.

For differential scanning calorimetry a Perkin–Elmer DSC-2 system was used. The scanning rates were 1·25, 2·5 and 20 K min^{-1}. The thermograms recorded at lower speeds indicated the transitions at 1–2 K less than their values from light microscopy. No attempt was made to correct the DSC values.

The X-ray powder diffraction recordings were obtained at room temperature using a Philips diffractometer and Cu–K_α radiation.

3. Results and discussion

3.1. *Optical study of phase transitions and morphologies*

When a polycrystalline specimen of BPC is gradually heated, it is often observed that a part of it melts at *c.* 330·5 K and the remainder at *c.* 338·5 K. Both the changes are to the nematic (N) phase, which passes to the isotropic (I) phase at *c.* 360 K. This melting behaviour is unusual and similar to that in some cyclohexane diesters [13]; it indicates the presence of two types of crystal in the original sample. Previous studies on BPC mention only a single melting at a temperature close to either of the values mentioned here [18, 19].

The N–I transition occurs without significant supercooling. But the nematic phase supercools by several degrees prior to crystallization. We used an isothermal mode of study to appreciate the crystallization process. When a liquid sample is suddenly introduced into the thermostatic stage at 300 K, crystallization is observed to follow in a few minutes. It is invariably spherulitic and the spherulites nucleate sporadically; often two morphologically different structures develop simultaneously, both of which are essentially two-dimensional, as evidenced by their large sizes (often several mm across). These may be referred to as the T (tangential) and R (radial) spherulites from the view point of molecular orientation (to be discussed later). The two melting points earlier mentioned belong to the T and R crystals, the latter being the higher melting variety. In figure 1 (*a*) showing the two types of spherulite, the central coarse structure without a well defined Maltese cross represents the T structure; the surrounding smaller formations that are compact and display the Maltese cross conspicuously are the R spherulites. The T morphology is initially sheaf-like and takes time to assume the circular shape; the R structure is disc-like even from the time it begins to appear. Both the spherulites have a linear growth rate (cf. figure 2) and their evolution is not therefore diffusion controlled [2]. The T spherulite is faster growing than the R, and the growth rates in both cases are temperature dependent (cf. figure 3), as in some polymers [7].

Optically both the R and T spherulites are positive as determined using a Berek compensator and thin (15 μm) samples. The T regions are less birefringent and show vivid interference colours as compared to the higher order pale colours in R regions.

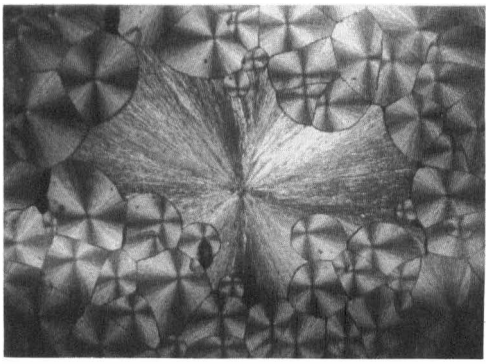

(*a*)

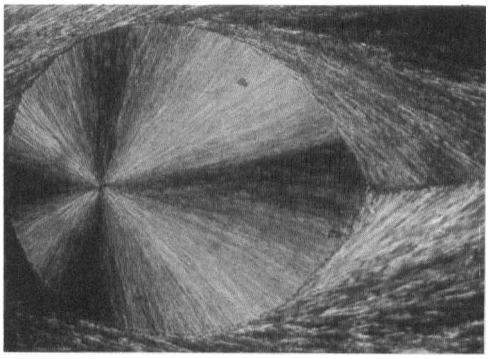

(*b*)

Figure 1. Two types of crystalline spherulite in a BPC film quenched from 373 K to 300 K, between crossed polarizers. (*a*) Central T type spherulite surrounded by R type spherulites, 75 μm sample, $\times$ 13. (*b*) An R spherulite enveloped by a faster growing T spherulite, 15 μm sample, $\times$ 45.

Within a given spherulite the colours vary from region to region as is to be expected of an assemblage of crystallites oriented randomly about the radial direction. It is important to note that the index ellipsoid characterizing the spherulites is the average formed by rotating the individual crystal ellipsoids randomly about the radial direction. Thus, even if the crystallites are themselves biaxial, the composite structure would be uniaxial.

As in the case of several mesogens [4], in BPC the mesomorphic fluid tends to inherit the textural features of the precursor phase. Thus even after the R and T spherulites melt, their morphology is largely maintained. Figure 4 shows this paramorphic feature for the R region. The absence of crystallinity is indicated here by the bright fluid at the zig–zag interspherulitic boundaries. It may be pointed out here that, in the crystalline state, cracks develop along the lines where the spherulites meet [1]. These 'boundary cracks', devoid mostly of the sample, appear dark between crossed polaroids. When the melting occurs the nematic fluid spreads out into these cracks, thus delineating the boundaries. These nematic domains maintain their outlines and the Maltese cross even upto the clearing point.

The molecular orientations in R and T spherulites could be readily deduced from the structure of their corresponding molten zones, R_N and T_N. By using 15 μm samples and a Berek compensator, we found the R_N and T_N zones to be positive and negative

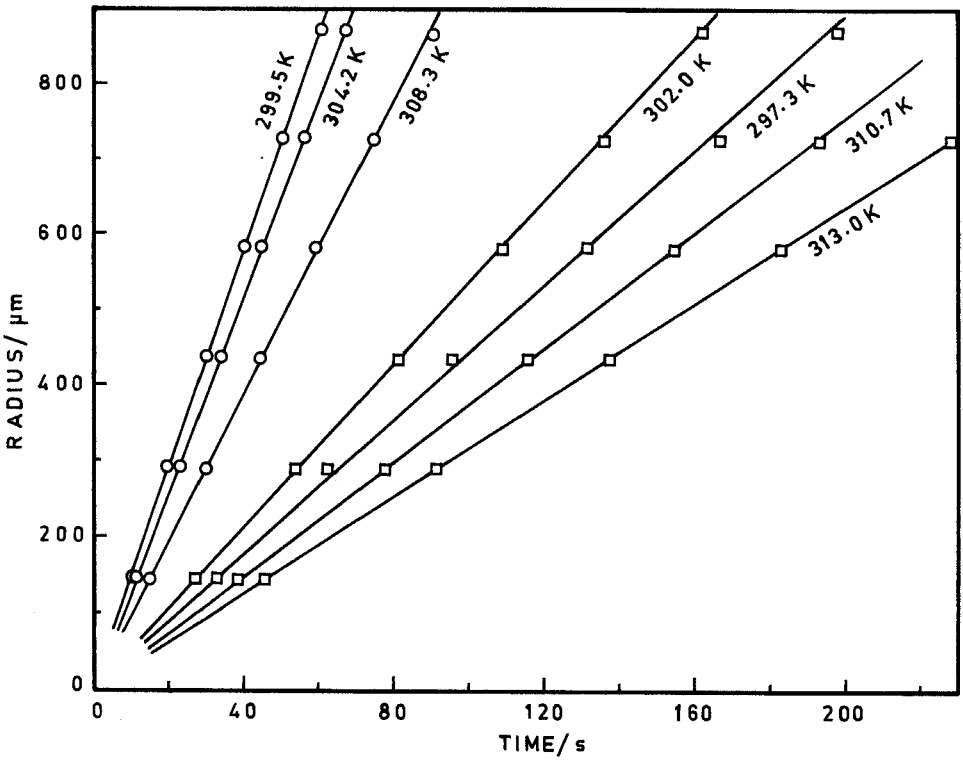

Figure 2. Dependence of radial growth on time for the R and T structures, at various temperatures, in a 75 μm sample. □, R spherulite; ○, T spherulite.

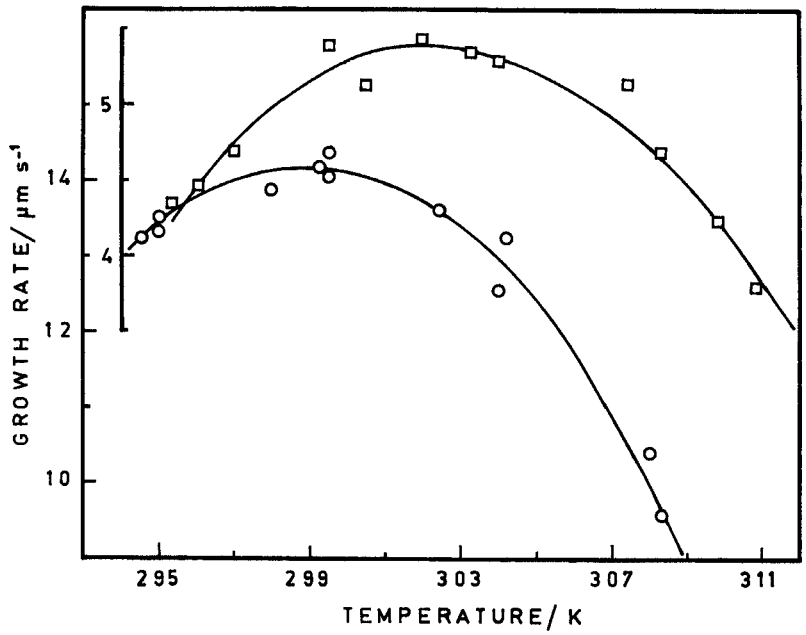

Figure 3. Growth rates of the spherulites in a 75 μm BPC sample as a function of crystallization temperature. □, R spherulite; ○, T spherulite.

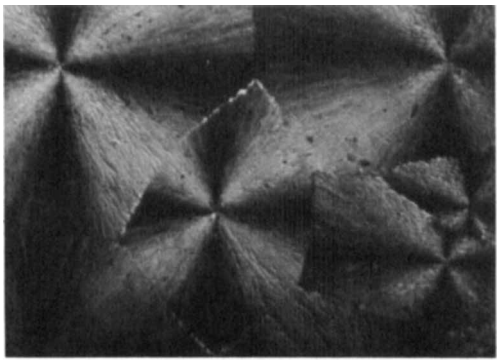

Figure 4. Persistence of spherulitic birefringence in the nematic state. An R_N region of a 75 μm sample at 339 K; crossed polarizers; $\times 45$.

respectively. In other words, the major molecular axes are radial in R_N and tangential in T_N. It may be clarified here that the opposite signs of crystalline and nematic spherulites, T and T_N, are not incompatible. The positive sign of the T spherulite could be explained by considering its crystallites to be biaxial. The refractive index of the crystallites along the spherulite radius, though may not be the largest of the indices, may become larger than the effective tangential index, because of the randomness of their orientation around the radial direction, as earlier noted. For example, if the crystallites are orthorhombic with their *b* axes along the spherulite radii, the refractive index n_β may be greater than the average of n_α and n_γ, to make the spherulite positive [20].

The nature of electric field induced domains in the nematic spherulites could also reveal the initial director patterns. Figures 5 and 6 show the results of the experiments using low frequency fields. In the R_N region, the focal lines due to the domains are predominantly circular (cf. figures 5 (*a*) and 6 (*a*)). By contrast, in the T_N region, the focal lines are largely radial (cf. figures 5 (*b*) and 6 (*b*)). Figures 6 (*c*) and (*d*) show the interferograms at two different voltages for a region where an R_N spherulite is surrounded by a T_N spherulite. Since it is known [21] that the focal lines of the Williams-like domain pattern run perpendicular to the optical axis in the field-off state, all these observations confirm the radial and tangential molecular alignments in the R_N and T_N aggregates.

Near the threshold voltage, the alignment distortion leading to Williams domains takes place periodically, in the plane of the electric field and the initial director [21]. Therefore, the periodic changes in refractive index experienced by the electric vector vibrating parallel to the optical axis of the undistorted specimen, will not be present for the vector perpendicular to the optical axis. This fact could be used to obtain additional evidence for the aforesaid molecular orientations in the spherulites (cf. figure 7).

We could also use the high frequency (> 5 kHz) field effects to deduce the molecular orientations. Such fields produce 'walls' in initially homogeneously aligned samples of BPC [16]. These walls are the transition regions between areas where the molecules are oppositely tilted during the Freedericksz deformation. Closed walls are unstable and their irregular initial geometry tends to become elliptical as they collapse. The ellipse will be oriented such that the major axis lies along the initial director orientation [16]. Interferograms of the walls in figure 8 confirm the molecular orientations in the R_N and T_N domains.

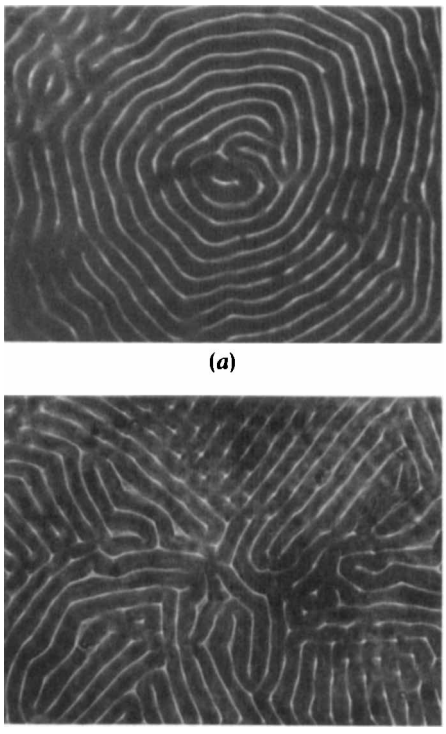

(*a*)

(*b*)

Figure 5. Virtual line images due to electric field induced domains in a 75 μm BPC film; 50 Hz; 7·6 V; 348 K; × 65. (*a*) Nearly circular domains in the nematic region obtained by melting an R spherulite. (*b*) Nearly radial domains in the nematic region obtained by melting a T spherulite.

Now we turn to isothermal crystallization above and below 300 K. The morphology of R depends on the degree of supercooling. When the temperature is 308 K, the R spherulites cease to show the Maltese cross and develop a dense branching morphology (cf. figure 9). Above *c.* 313 K, nematic BPC remains undercooled indefinitely. To examine the nature of secondary nucleation at higher temperatures, samples just melted to the liquid could be briefly exposed to the ambient and then introduced into the hot stage kept at the required temperature. During exposure to the ambient, a few R and T structures nucleate. They develop slightly during the process of attaining thermal equilibrium in the hot stage. Then the growth of R is arrested if the temperature is over 315 K. Further crystallization occurs in a non-spherulitic, lamellar way. The lamellar (L) crystals originate only at the R boundaries, but not the T boundaries. The L crystals are leaf-like to begin with (cf. figures 10(*a*) to (*d*)), and are extinct between crossed polarizers when their long dimension is along the axis of either polarizer. They overlap (cf. figure 10(*b*)) and grow outward to eventually fill the sample volume (cf. figure 10(*d*)). Optically, the L crystals are positive. Under conoscopic examination, they usually present the centred acute bisectrix interference figure which gives the apparent optic angle, $2E$, as *c.* 99·5°. Since the L crystals grow from the R boundaries, they may belong to the same crystal class as the crystallites of R.

T spherulites do not form above 313 K. Their texture above 308 K consists of a coarse centre; but the growth front away from the centre is constituted of clear, wide

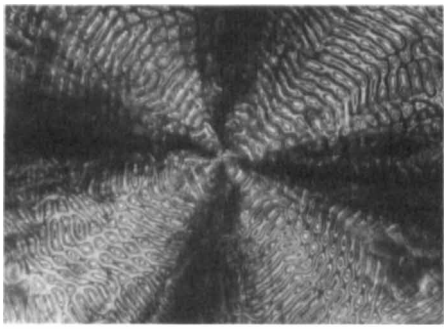

(*a*)

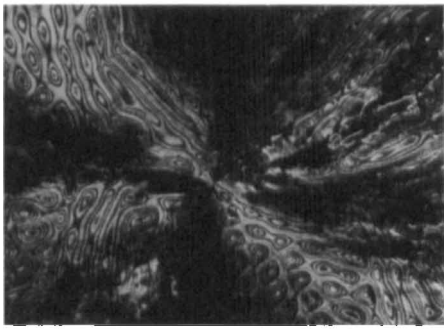

(*b*)

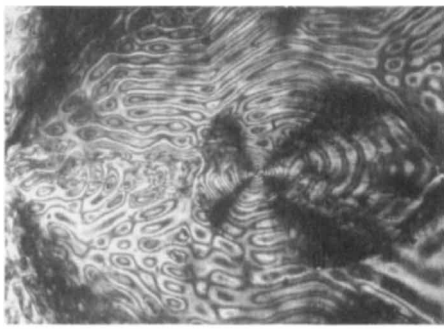

(*c*)

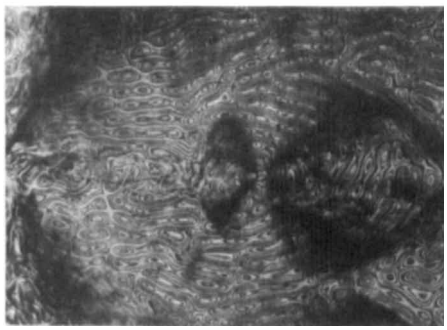

(*d*)

Figure 6. Interferograms in the paramorphic nematic regions, obtained with mercury green light. (*a*) R_N region, 9·3 V, 347 K; (*b*) T_N region, 6·7 V, 343·5 K; (*c*) R_N region within T_N, 8·3 V, 352 K; and (*d*) same area as in (*c*), 9·5 V, 50 Hz, × 50.

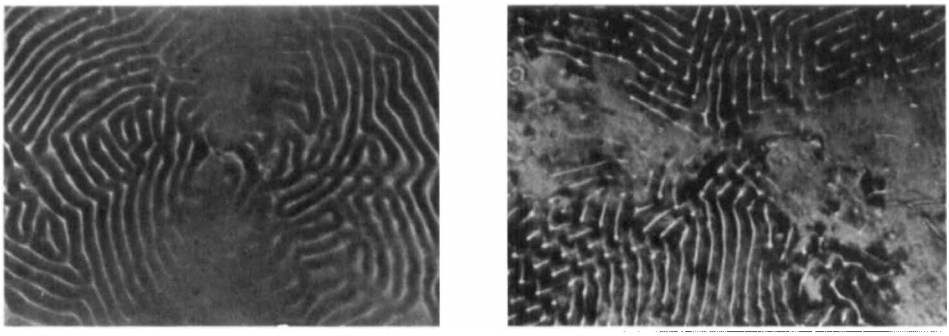

(*a*) (*b*)

Figure 7. Domains in a 75 μm film viewed with a single polarizer set with its transmission axis parallel to the longer edge of the figure. Paramorphic areas obtained by melting (*a*) an R spherulite and (*b*) a T spherulite. Virtual images, 8·5 V, 344 K, 30 Hz, $\times$ 45.

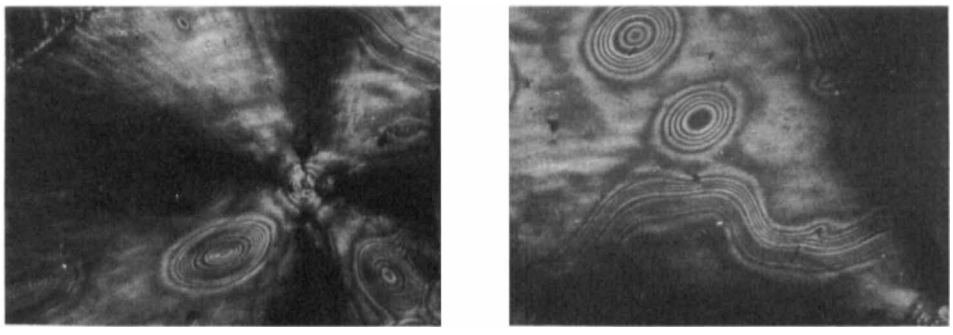

(*a*) (*b*)

Figure 8. Interferograms of the elliptical walls in the paramorphic areas, obtained using mercury green light, 348 K. (*a*) R_N region, 20 kHz, 16·2 V, $\times$ 50. (*b*) T_N region 10 kHz, 14 V, $\times$ 56; spherulite centre is at the lower righthand corner and the two arms of the Maltese cross are along the edges.

and arrow headed crystallites. Conoscopic observation of these crystallites reveals them to be biaxial and positive. The angle 2*E* could not be measured although centred acute bisectrix figures were seen, since the melatopes were just outside the visual range.

Preliminary studies of crystallization at lower temperatures have shown that, between 278 and 300 K, the aggregation is spherulitic. The R and T organizations occur simultaneously. In addition, another type of externally symmetrical aggregation is noticed. The corresponding texture comprises very dark, roundish objects (cf. figure 11). The darkness is due to light scattering, and the objects appear as white specks in direct reflected light.

3.2. *X-ray diffraction*

Several phenyl benzoates with O*R* (*R* = Alkyl) and O.CO.*R*′ or CO.*R*′ as the end groups form both N and S (smectic) phases [13, 14]. This could lead one to consider the possibility of the spherulites in BPC being smectic rather than crystalline. However, the S phase is unlikely because of the remarkable undercooling of the transition to the 'spherulite phase' [22, 23]. The typical crystalline morphology of the spherulites and their mechanical rigidity are the other factors on which we have based the phase assignment.

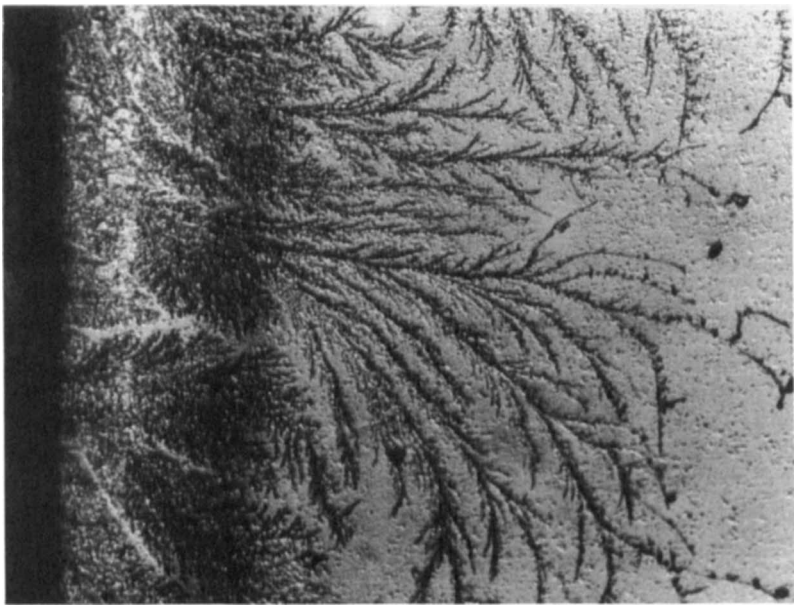

Figure 9. Dense branching morphology of an R spherulite (dark area to the left) extending beyond the coverslip where only a trace of the film is present. Natural light, 308 K, × 70.

The X-ray diffraction patterns of the R and T powder specimens would also appear to be consistent with the crystalline nature of the spherulites. The patterns in figure 12 clearly show that the two structures are associated with different 3D lattices. The distinguishing feature of the S phases, namely the low angle reflection (near $2\Theta = 3{\cdot}5°$), is absent in the pattern for R. Hence the R structure is probably crystalline, with an interdigitated arrangement of molecules. The pattern for T shows a low angle line corresponding to 2·47 nm, which is almost equal to the length of the BPC molecule (as estimated from the molecular length for similar esters [24]). It seems also possible to identify a few higher order reflections corresponding to the long spacing. Thus a layer lattice, with the molecules orthogonal to the layer planes, is likely for T. Since the T crystallites are optically biaxial, the smectic type to be considered for T is only S_E. However, bimesomorphism involving $S_E N$ combination is rather unlikely [23]. Further X-ray work is necessary in order to make a definite choice between the highly ordered smectic and crystal phases.

3.3. *Differential scanning calorimetry*

The DSC thermograms of BPC are given in figures 13 and 14. The first heating (cf. figure 13, scan A), shows two strong endothermic peaks near 328·3 and 337·6 K and a mild peak at 358·1 K. These correspond respectively to T–N, R–N and N–I transformations. On cooling (cf. figure 13, scan B), the N–crystal transition, which undercools significantly, becomes noticeable only at *c.* 304 K. This exotherm extends down to about 285 K, indicating a sporadic development of crystalline spherulites. During reheating (cf. figure 13, scan C), a mild peak corresponding to the T–N change and an intense peak due to the R–N change are observed. During the first cooling, therefore, most of the sample must have crystallized in the R form. From the heating runs with the R and T samples taken separately, the enthalpy changes ΔH_{RN} and ΔH_{TN} have been estimated to be *c.* 23·4 and 31·8 kJ mol^{-1}, respectively.

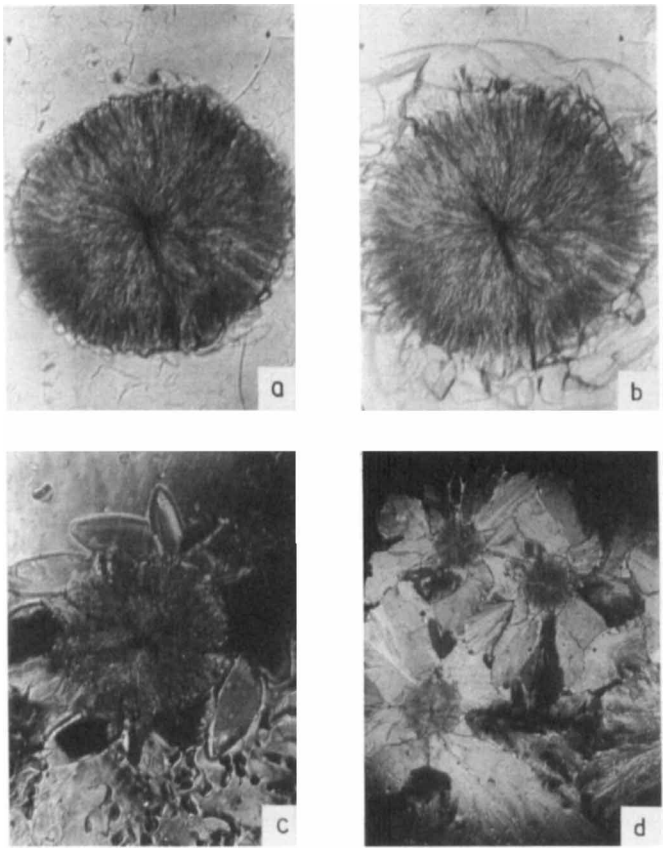

Figure 10. Growth of lamellar (L) crystals from the boundaries of 'seed' spherulites of R type, at higher temperatures, in a 75 μm sample; (*a*) and (*b*) textures in natural light, 324·5 K, × 57; (*c*) texture after 18 min of insertion of the sample in the hot stage, crossed polarizers set diagonally, 324 K, × 35; (*d*) texture at the end of crystallization at 317 K, crossed polarizers, × 10·5.

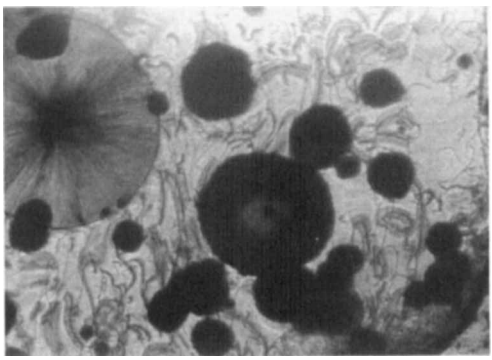

Figure 11. Texture of BPC at 280 K, showing several dark, roundish crystalline aggregates. Natural light, × 42.

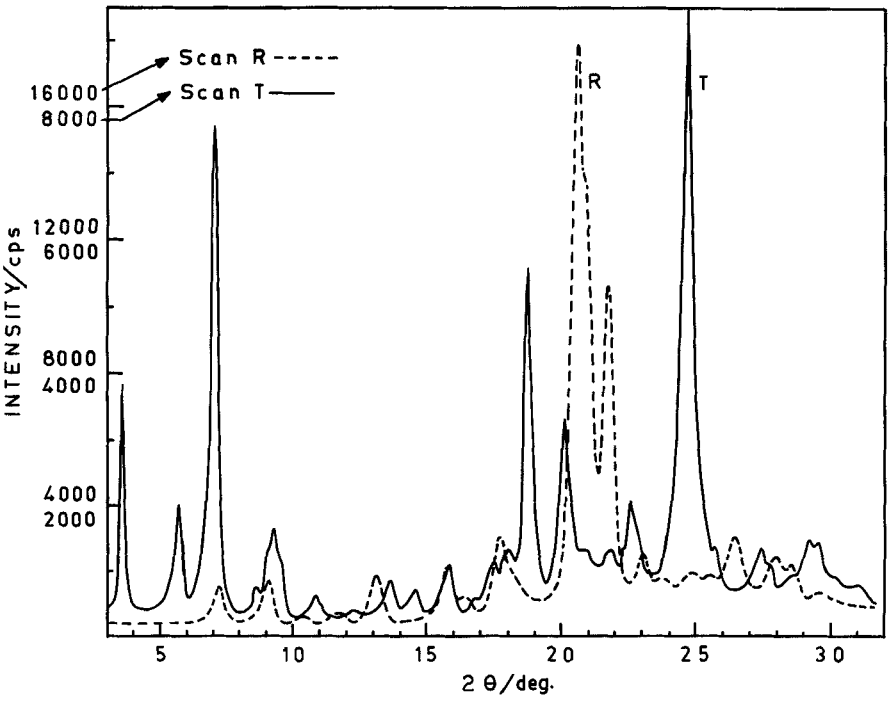

Figure 12. X-ray diffractometer recordings for the R and T powder specimens, obtained with Cu–K_α radiation at room temperature.

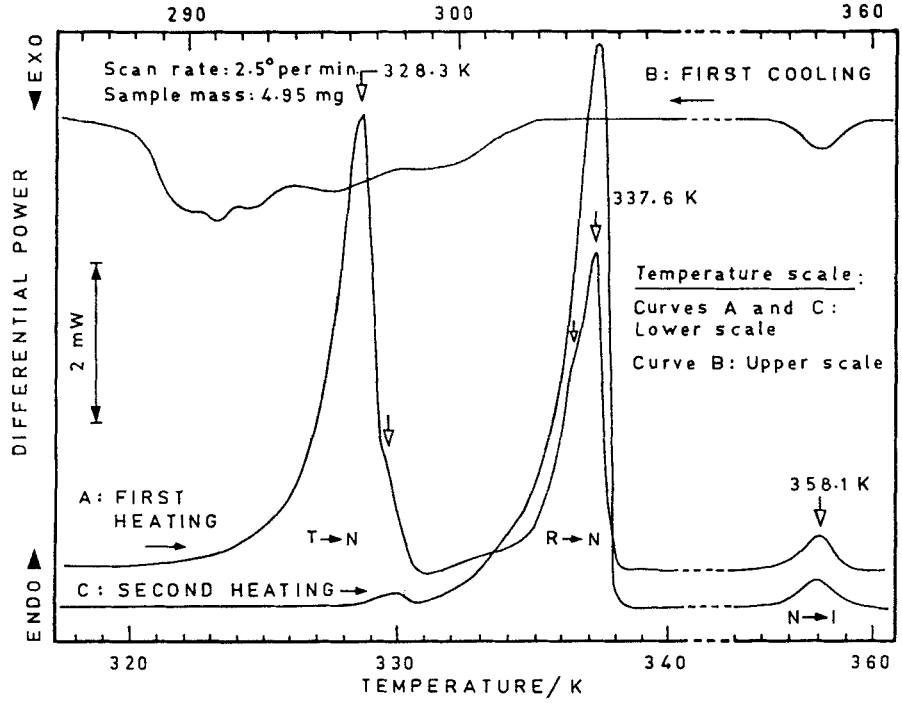

Figure 13. DSC thermograms of BPC.

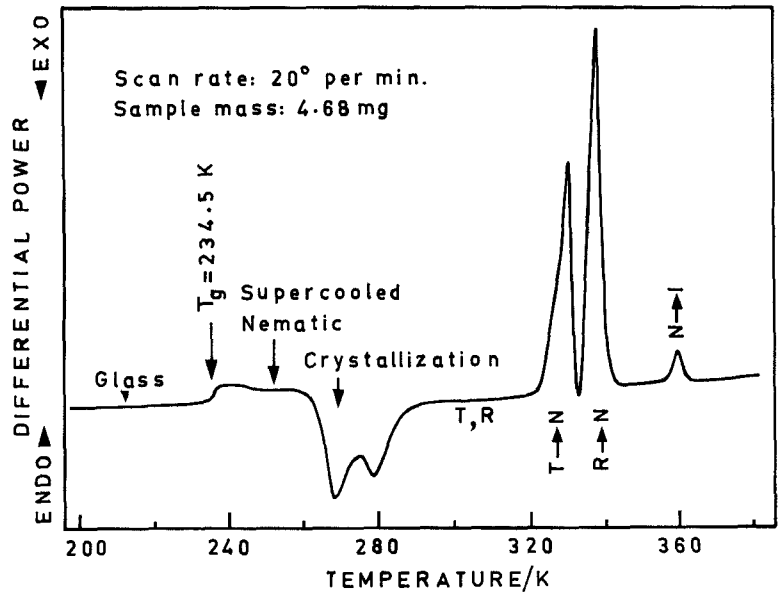

Figure 14. DSC thermograms of BPC showing the existence of the glassy nematic state.

Figure 14 shows the thermogram for a heating run at 20 K min^{-1} on a sample initially cooled from 365 K to 110 K at the rate of 80 K min^{-1}. The main feature here is the transition from the glassy nematic to the supercooled nematic state, taking place at about 234·5 K. Similar glass transition phenomena have been observed earlier in several other mesogens [25]. Figure 14 shows that the crystallization from the strongly supercooled nematic state involves both the R and T modifications.

It seems significant to note that in figure 13, the curves A and C show the T–N and R–N peaks to be unresolved doublets; the first has a shoulder on the high temperature side, and the second on the low temperature side. These are not impurity effects, since in some experiments the shoulders in figure 13 appear as the main peaks and vice versa. For instance, in figure 14 the peak for the T–N change has a shoulder on the low temperature side. Hence it is possible that each of the doublets arises due to two types of solid; but no definite optical evidence could be found to support this conclusion.

We are grateful to the Commandant, College of Military Engineering for his keen interest in this investigation. We are indebted to Dr. K. Usha Deniz, Bhabha Atomic Research Centre, for the DSC facility and to M/s Eastman Organic Chemicals for the supply of samples of BPC.

References

[1] Geil, P. H., 1963, *Polymer Single Crystals* (Wiley–Interscience), Chap. IV.
[2] Mandelkern, L., 1964, *Crystallization in Polymers* (McGraw-Hill), Chap. 9.
[3] Goldenfeld, N., 1987, *J. Crystal Growth*, **84**, 601.
[4] Kelker, H., and Hatz, R., 1980, *Handbook of Liquid Crystals* (Verlag Chemie), p. 24.
[5] Price, F. P., and Wendorff, J. H., 1971, *J. phys. Chem.*, **75**, 2839 and 2849; 1972, *J. Phys. Chem.*, **76**, 276.
[6] Price, F. P., and Fritzsche, A. K., 1973, *J. phys. Chem.*, **77**, 396.
[7] Adamski, P., Dylik-Gromiec, A., Klimczyk, S., and Wojciechowski, M., 1976, *Molec. Crystals liq. Crystals*, **35**, 171.

[8] ADAMSKI, P., and KLIMCZYK, S., 1978, *Sov. Phys. Crystallogr.*, **23,** 82.
[9] ADAMSKI, P., and CZYZEWSKI, R., 1978, *Sov. Phys. Crystallogr.*, **23,** 725.
[10] ADAMSKI, P., DYLIK-GROMIEC, A., and WOZJCIECHOWSKI, M., 1981, *J. Crystal Growth*, **52,** 332.
[11] BLUMSTEIN, R. B., POLIKS, M. D., STICKLES, E. M., BLUMSTEIN, A., and VOLINO, F., 1985, *Molec. Crystals liq. Crystals*, **129,** 375.
[12] OZCAYIR, Y., and BLUMSTEIN, A., 1986, *Molec. Crystals liq. Crystals*, **135,** 237.
[13] NEUBERT, M. E., HERLINGER, F. C., JIROUSEK, M. R., and DE VRIES, A., 1986, *Molec. Crystals liq. Crystals*, **139,** 299.
[14] NEUBERT, M. E., WILDMAN, P. J., ZAWASKI, M. J., HANLON, C. A., BENYO, T. L., and DE VRIES, A., 1987, *Molec. Crystals liq. Crystals*, **145,** 111.
[15] KRISHNAMURTHY, K. S., 1984, *Jap. J. appl. Phys.*, **23,** 1165.
[16] KRISHNAMURTHY, K. S., and BHATE, M. S., 1985, *Molec. Crystals liq. Crystals*, **128,** 29.
[17] GRAY, G. W., 1962, *Molecular Structure and Properties of Liquid Crystals* (Academic), p. 59.
[18] BONNE, U., and CUMMINGS, J. P., 1972, *Properties and Limitations of Liquid Crystals for Aircraft Displays* (Honeywell Inc.), p. 13.
[19] DE JEU, W. H., and LATHOUWERS, TH. W., 1974, *Molec. Crystals liq. Crystals*, **26,** 225.
[20] HAUDIN, J. M., 1986, *Optical Properties of Polymers*, edited by G. H. Meeten (Elsevier), p. 180.
[21] PENZ, P. A., 1970, *Phys. Rev. Lett.*, **24,** 1405; 1972 *Phys. Rev.* A, **6,** 414.
[22] DE VRIES, A., 1973, *Pramana*, Suppl. **1,** 111.
[23] DEMUS, D., DIELE, S., GRANDE, S., and SACKMANN, H., 1983, *Advances in Liquid Crystals*, Vol. 6, edited by G. H. Brown (Academic), p. 1.
[24] NEUBERT, M. E., LEUNG, K., and SAUPE, A., 1986, *Molec. Crystals liq. Crystals*, **135,** 283.
[25] SORAI, M., NAKAMURA, T., and SEKI, S., 1975, *Pramana*, Suppl. **1,** 503.